

Substituent Effects on an Antibody-Catalyzed Hydrolysis of Phenyl Esters: Further Evidence for an Acyl-Antibody Intermediate

Richard A. Gibbs,^{†,§} Patricia A. Benkovic,[†] Kim D. Janda,[‡] Richard A. Lerner,[‡] and Stephen J. Benkovic^{*†}

Contribution from the Department of Chemistry, The Pennsylvania State University, 152 Davey Laboratory, University Park, Pennsylvania 16802, and Departments of Molecular Biology and Chemistry, Scripps Clinic and Research Institute, 10666 North Torrey Pines Road, La Jolla, California 92037. Received August 28, 1991

Abstract: The hydrolysis of a series of para-substituted phenyl esters (**2** and **6a-d**) by the monoclonal catalytic antibody NPN43C9 has been investigated. The apparent pK_a observed in the k_{cat}/K_m -pH profiles shifts from 8.9 (*p*-nitrophenyl ester) up to a maximum of 9.5 (*p*-methylphenyl ester). A correlation of the antibody-catalyzed rates of hydrolysis of the esters versus the σ parameter affords a ρ value of 2.3, indicative of a hydrolytic mechanism proceeding via the attack of a neutral nitrogen nucleophile and contrasting with the low ρ value expected for general base catalyzed hydrolysis. There was an inverse solvent deuterium isotope effect on the antibody-catalyzed hydrolysis of the *p*-chlorophenyl ester at pH > 10. These observations are consistent with our previous proposal (Benkovic, et al. *Science* 1990, 250, 1135) that this antibody employs a multistep kinetic pathway which involves the formation of a covalent acyl-antibody intermediate.

Introduction

Since the first reports in 1986 that certain antibodies catalyzed the hydrolysis of esters and carbonates, it has been demonstrated that a veritable panoply of chemical transformations is amenable to antibody catalysis.¹ However, there has been a relative paucity of detailed studies on the manner in which these antibodies perform their catalytic function.²⁻⁷ Such studies are important because they can provide insight into how to produce improved catalytic antibodies. In addition, these studies are of interest because they illuminate the similarities and differences between antibodies and enzymes. In this paper, we report the results of further mechanistic studies on the antibody NPN43C9, which hydrolyzes an amide bond in the *p*-nitroanilide **1** (Figure 1).⁸ These studies provide additional support for our proposal that this antibody employs a multistep kinetic pathway which involves a covalent acyl-antibody intermediate.²

The results of a combination of steady-state and pre-steady-state kinetic experiments on the hydrolysis of the anilide **1** and *p*-nitro ester **2** by NPN43C9 have been recently described.² Particularly instructive were the pH-rate profiles for substrates **1** and **2** which both exhibited an apparent pK_a of 9.0. This would appear to be consistent with a catalytic group in the antibody binding pocket (presumably acting as a general base) with a pK_a of \sim 9. However, solvent isotope effect studies on the hydrolysis of amide **1** were not consistent with this interpretation. The pK_a in D₂O shifts to \sim 10 (a much larger change than is seen with normal acids), suggesting that the observed pK_a is due to a change in the rate determining step, and there is no measurable solvent isotope effect on k_{cat} in the pH independent region.³ Furthermore, k_{cat} for ester **2** at pH > 9 is limited by release of the *p*-nitrophenol product, suggesting that the pK_a in the ester k_{cat} -pH profile is also an apparent one due to a change in rate limiting step. Neither the rate constant for release of *p*-nitrophenol nor the thermodynamic binding constant for association of the anilide substrate were pH sensitive over the observational pH range. As a result of these findings, a kinetic scheme was proposed for the antibody which involves the rapid yet unfavorable formation of an acyl-antibody intermediate, followed by its hydroxide-mediated hydrolysis to afford the product acid and phenol or aniline. In this study, the hydrolysis of a series of para-substituted phenyl esters by

NPN43C9 has been investigated.

There are four specific items of information that we hoped to obtain from a substituent effect study. First, we wanted to determine whether the antibody would bind to and hydrolyze the para-substituted analogues of the *p*-nitrophenyl ester. Previous studies in this laboratory have shown that catalytic antibodies are quite specific with respect to their substrates. Therefore it was of interest to ascertain what type of latitude the antibody would allow in substitutions at the para position. Secondly, we hoped to find an ester for which chemistry rather than product release was rate limiting at pH > 9, in contrast to the behavior of the *p*-nitro ester **2** (for which *p*-nitrophenol release is rate limiting at high pH). Thirdly, if a variety of para-substituted esters were hydrolyzed by NPN43C9, then a correlation of the σ values for the para substituents with the rates of antibody-catalyzed hydrolysis might provide evidence about the nature of the rate limiting step. Finally, if the pK_a of \sim 9 in the pH-rate profiles is due to a change in rate limiting step from deacylation (pH < 9) to acylation or product release (pH > 9), then the relative rates of these steps should change as the leaving group on the ester is varied, and the observed pK_a should change. In this paper we report the results of the interactions of six homologous phenyl esters (**2** and **6a-e**) with the antibody NPN43C9.⁹ In addition, we have investigated the hydrolysis of the *m*-nitroester **8** and *p*-chloroanilide **9** by NPN43C9.

Experimental Section

Synthesis of Esters 6a-e and 8 and Amide 9. Figure 3 depicts the synthetic route used to prepare the alternate substrates. A representative

(1) Lerner, R. A.; Benkovic, S. J.; Schultz, P. G. *Science* 1991, 252, 659-667.

(2) Benkovic, S. J.; Adams, J. A.; Borders, C. L., Jr.; Janda, K. D.; Lerner, R. A. *Science* 1990, 250, 1135-1139.

(3) Janda, K. D.; Ashley, J. A.; Jones, T. M.; McLeod, D. A.; Schloeder, D. M.; Weinhouse, M. I.; Lerner, R. A.; Gibbs, R. A.; Benkovic, P. A.; Hilhorst, R.; Benkovic, S. J. *J. Am. Chem. Soc.* 1991, 113, 291-297.

(4) Wirsching, P.; Ashley, J. A.; Benkovic, S. J.; Janda, K. D.; Lerner, R. A. *Science* 1991, 252, 680-685.

(5) Tramontano, A.; Ammann, A. A.; Lerner, R. A. *J. Am. Chem. Soc.* 1988, 110, 2282-2286.

(6) Jackson, D. Y.; Prudent, J. R.; Baldwin, E. P.; Schultz, P. G. *Proc. Natl. Acad. Sci. U.S.A.* 1991, 88, 58-62.

(7) Martin, M. T.; Napper, A. D.; Schultz, P. G.; Rees, A. R. *Biochemistry* 1991, 30, 9757-9761.

(8) Janda, K. D.; Schloeder, D.; Benkovic, S. J.; Lerner, R. A. *Science* 1988, 241, 1188-1191.

(9) Previously, we have reported that NPN43C9 can hydrolyze **6c**: Gibbs, R. A.; Posner, B. A.; Filipula, D. R.; Dodd, S. W.; Finkelman, M. A. J.; Lee, T. K.; Wroble, M.; Whitlow, M.; Benkovic, S. J. *Proc. Natl. Acad. Sci. U.S.A.* 1991, 88, 4001-4004.

[†] The Pennsylvania State University.

[‡] Scripps Clinic and Research Institute.

[§] Recipient of NSF Postdoctoral Fellowship CHE-8808377. Current address: Department of Pharmaceutical Sciences, College of Pharmacy and Allied Health Professions, Wayne State University, 528 Shaper Hall, Detroit, MI 48202.

procedure for the synthesis of the *m*-nitroester **8** is given below. To a clear yellow solution of acid **10**^{10a} (251 mg, 1.00 mmol) and *m*-nitrophenol (209 mg, 1.50 mmol) in ethyl acetate (5 mL) was added EDC (1-(3-dimethylaminopropyl)-3-ethylcarbodiimide hydrochloride, Aldrich Chemical Co., 229 mg, 1.20 mmol). The resulting suspension was stirred for 24 h at room temperature, and then taken up in ethyl acetate (~50 mL). The organic layer was then washed with 1 N aqueous HCl (3 × 20 mL) and water (~20 mL), dried (MgSO₄), filtered and concentrated. Purification by flash chromatography (3 × 15 cm silica gel, 30% ethyl acetate in hexanes) afforded 290 mg (78%) of the desired ester **11** (R = *m*-NO₂C₆H₄O) as a brown solid: ¹H NMR (360 MHz, CDCl₃) δ 8.12 (ddd, *J* ~ 8.2, 2.3, 0.8 Hz, 1 H), 7.97 (app t, *J* ~ 2.3 Hz, 1 H), 7.54 (app t, *J* ~ 8.2 Hz, 1 H), 7.42 (ddd, *J* ~ 8.2, 2.3, 0.8 Hz, 1 H), 7.39 and 7.30 (two d, AB pattern, *J* ~ 7.5 Hz, 4 H), 6.55 (s, 1 H), 3.60 (s, 2 H), 1.50 (s, 9 H) [For (R = *p*-CH₃COC₆H₄O) ¹H NMR (300 MHz, CDCl₃) δ 7.9 (d, *J* ~ 3.0 Hz, 2 H), 7.4 (d, *J* ~ 3.0 Hz, 2 H), 7.3 (d, *J* ~ 3.0 Hz, 2 H), 7.1 (d, *J* ~ 3.0 Hz, 2 H), 6.6 (s, 1 H), 3.8 (s, 2 H), 2.6 (s, 3 H), 1.50 (s, 9 H); for (R = *p*-CHOC₆H₄O) ¹H NMR (300 MHz, CDCl₃) δ 10.0 (s, 1 H), 7.4–7.25 (m, 6 H), 7.0 (d, *J* ~ 9.0 Hz, 2 H), 6.5 (br s, 1 H), 3.8 (s, 2 H), 1.50 (s, 9 H); for (R = *p*-ClC₆H₄O) ¹H NMR (300 MHz, CDCl₃) δ 7.9 (d, *J* ~ 3.0 Hz, 2 H), 7.4 (d, *J* ~ 3.0 Hz, 2 H), 7.3 (d, *J* ~ 3.0 Hz, 2 H), 7.1 (d, *J* ~ 3.0 Hz, 2 H), 7.0 (d, *J* ~ 3.0 Hz, 2 H) 6.5 (br s, 1 H), 3.8 (s, 2 H), 1.52 (s, 9 H); for (R = *p*-CH₃C₆H₄O) ¹H NMR (300 MHz, CDCl₃) δ 7.5–7.3 (m, 4 H), 7.2 (d, *J* ~ 2.5 Hz, 2 H), 6.9 (d, *J* ~ 2.5 Hz, 2 H), 6.6 (s, 1 H), 3.8 (s, 2 H), 2.4 (s, 3 H), 1.50 (s, 9 H); for (R = C₆H₅O) ¹H NMR (300 MHz, CDCl₃) δ 7.4–6.9 (m, 9 H), 6.5 (br s, 1 H), 3.8 (s, 2 H), 1.6 (s, 9 H); for (R = *p*-ClC₆H₄NH) ¹H NMR (360 MHz, acetone-*d*₆) δ 9.33 (br s, 1 H), 8.3 (br s, 1 H), 7.62 (d, *J* ~ 8.9 Hz, 2 H), 7.46 (d, *J* ~ 8.5 Hz, 2 H), 7.25 (d, *J* ~ 8.9 Hz, 2 H), 7.21 (d, *J* ~ 8.5 Hz, 2 H), 3.6 (s, 2 H), 1.45 (s, 9 H)]. To a solution of Boc-protected ester **11** (R = *m*-NO₂C₆H₄O) (110 mg, 0.25 mmol) in dichloromethane (10 mL, HPLC grade) was added trifluoroacetic acid (3.0 mL, distilled from KMnO₄). After 1 h at room temperature, TLC analysis (5% methanol/CHCl₃, developed with ninhydrin) indicated that the starting material had been completely converted into the amine **12** (R = *m*-NO₂C₆H₄O). The solvent was removed, and the amine was dried under high vacuum and then taken up in dichloromethane. Glutaric anhydride (34 mg, 0.30 mmol) and triethylamine (0.041 mL, 0.30 mmol) was added, and the resulting cloudy mixture was stirred at room temperature for 2 h. The reaction mixture was then concentrated and purified by flash chromatography (10% methanol/CHCl₃, 2 × 15 cm silica gel) to afford 34 mg (36%) of the desired ester **8**. Analytically pure material was obtained by reversed phase HPLC purification. The chromatographic system consisted of a Waters 600E solvent delivery module equipped with a Waters 484 UV-visible detector (monitoring at 254 nm), a Hewlett-Packard 3394A integrator, and a Whatman ODS reversed phase semipreparative column (9.4 mm × 50 cm). A flow rate of 4 mL/min was used with a linear gradient of 95% water to 95% CH₃CN over 30 min. The retention time of the *m*-nitro ester **8** was 23.0 min: ¹H NMR (360 MHz, CD₃OD) δ 8.12 (ddd, *J* ~ 8.2, 2.3, 0.8 Hz, 1 H), 7.97 (app t, *J* ~ 2.3 Hz, 1 H), 7.62 (app t, *J* ~ 8.2 Hz, 1 H), 7.48 (ddd, *J* ~ 8.2, 2.3, 0.8 Hz, 1 H), 7.55 and 7.32 (two d, AB pattern, *J* ~ 7.5 Hz, 4 H), 3.92 (s, 2 H), 2.40 (m, 4 H), 2.0 (m, 2 H). Anal. Calcd for C₁₉H₁₈O₅N₂: C, 59.06; H, 4.70; N, 7.25. Found: C, 55.09; H, 4.79; N, 7.35.^{10b} For **6a**: ¹H NMR (300 MHz, CD₃OD) δ 8.1 (d, *J* ~ 3.0 Hz, 2 H), 7.6 (d, *J* ~ 3.0 Hz, 2 H), 7.3 (d, *J* ~ 3.0 Hz, 2 H), 7.2 (d, *J* ~ 3.0 Hz, 2 H), 3.9 (s, 2 H), 2.6 (s, 3 H), 2.5–2.3 (m, 4 H), 2.1–1.9 (m, 2 H). Anal. Calcd for C₂₁H₂₁O₆N: C, 65.79; H, 5.52; N, 3.65. Found: C, 64.49; H, 5.66; N, 3.20. For **6b**: ¹H NMR (300 MHz, DMSO-*d*₆) δ 10.0 (s, 1 H), 9.9 (s, 1 H), 7.98 (d, *J* ~ 9 Hz, 2 H), 7.55 (d, *J* ~ 9 Hz, 2 H), 7.36 (d, *J* ~ 9 Hz, 2 H), 7.3 (d, *J* ~ 9.0 Hz, 2 H), 3.95 (s, 2 H), 2.35 (t, *J* ~ 8.0 Hz, 2 H), 2.25 (t, *J* ~ 8.0 Hz, 2 H), 1.8 (m, 2 H). Anal. Calcd for C₂₀H₁₉O₆N: C, 65.03; H, 5.18; N, 3.79. Found: C, 58.89; H, 5.07; N, 2.49.^{10b} For **6c**: ¹H NMR (300 MHz, DMSO-*d*₆) δ 9.9 (s, 1 H), 7.57 (d, *J* ~ 9.0 Hz, 2 H), 7.48 (d, *J* ~ 9.0 Hz, 2 H), 7.29 (d, *J* ~ 9.0 Hz, 2 H), 7.18 (d, *J* ~ 9.0 Hz, 2 H), 3.9 (s, 2 H), 2.32 (t, *J* ~ 8.0 Hz, 2 H), 2.26 (t, *J* ~ 8.0 Hz, 2 H), 1.8 (m, 2 H). Anal. Calcd for C₁₉H₁₈ClO₅N: C, 60.75; H, 4.83; N, 3.73. Found: C, 60.96; H, 4.94; N, 3.78. For **6d**: ¹H NMR (300 MHz, CD₃OD) δ 7.6 (d, *J* ~ 2.5 Hz, 2 H), 7.4 (d, *J* ~ 2.5 Hz, 2 H), 7.2 (d,

J ~ 2.5 Hz, 2 H), 6.9 (d, *J* ~ 2.5 Hz, 2 H), 3.9 (s, 2 H), 2.6–2.4 (m, 4 H), 2.4 (s, 3 H), 2.1–1.7 (m, 2 H). Anal. Calcd for C₂₀H₂₁O₅N: C, 67.58; H, 5.96; N, 3.94. Found: C, 67.01; H, 5.89; N, 3.82. For **6e**: ¹H NMR (300 MHz, CD₃OD) δ 7.4–6.9 (m, 9 H), 3.9 (s, 2 H), 2.6–2.4 (m, 4 H), 2.1–1.9 (m, 2 H). Anal. Calcd for C₁₉H₁₉O₅N: C, 66.85; H, 5.61; N, 4.10. Found: C, 66.91; H, 5.68; N, 4.12. For **9**: ¹H NMR (360 MHz, CD₃OD) δ 7.54 (d, *J* ~ 8.4 Hz, 2 H), 7.51 (d, *J* ~ 8.4 Hz, 2 H), 7.28 (d, *J* ~ 8.4 Hz, 4 H), 3.6 (s, 2 H), 2.5–2.3 (m, 4 H), 2.0–1.9 (m, 2 H). Anal. Calcd for C₁₉H₁₉ClO₄N₂: C, 60.88; H, 5.11; N, 7.48. Found: C, 60.62; H, 5.09; N, 7.13.

Steady-State Kinetics. Initial velocities for the monoclonal antibody NPN43C9 catalyzed hydrolyses of esters **6a–d** were determined by measuring the increase in absorbance due to production of phenols **7a–d**. The isosbestic wavelengths used to follow the hydrolyses were as follows: 292.5 nm ($\epsilon = 7730 \text{ M}^{-1}$) for *p*-hydroxyacetophenone **7a**; 300 nm ($\epsilon = 15050 \text{ M}^{-1}$) for *p*-hydroxybenzaldehyde **7b**; 282 nm ($\epsilon = 1392 \text{ M}^{-1}$) for *p*-chlorophenol **7c**; and 280 nm ($\epsilon = 1420 \text{ M}^{-1}$) for *p*-methylphenol **7d**. The 1-mL reaction mixtures contained 0.1–1.0 μM monoclonal antibody NPN43C9, 100–2500 μM of the appropriate ester, and 2.5% DMF in ATC buffer [0.1 M Aces (*N*-(2-acetamido)-2-aminoethanesulfonic acid), 0.05 M Tris, 0.05 M Caps (3-(cyclohexylamino)-1-propanesulfonic acid)], and each reaction was initiated by addition of the substrate at 25 °C. The initial velocities obtained were corrected for the rate of the background reaction. The K_m and k_{cat} values were determined by fitting the initial velocities to the Michaelis-Menten equation using the Kintastat program (an adaptation of Cleland's program¹¹ for the Macintosh microcomputer). The K_i values for phenols **7b** and **7c** were determined from their ability to inhibit the hydrolysis of **6c** by NPN43C9. The data obtained were then fit to a competitive inhibition model.¹¹

The steady-state kinetics for the hydrolysis of the *m*-nitrophenyl ester **8** by antibody NPN43C9 were determined by stopped flow spectrophotometry due to product inhibition by *m*-nitrophenol (vide infra), which resulted in curved initial reaction plots when manual mixing was used. Equal volumes of the ester **8** (100–500 μM) in 5% DMF (v/v)/5 mM Aces (pH 4.0) and NPN43C9 (1.0 μM) in 2X ATC, pH 9.6 were mixed together in an Applied Photophysics stopped flow spectrometer (final buffer concentration: 103 mM Aces, 50 mM Tris, 50 mM Caps; final substrate concentrations: 50–250 μM ; final NPN43C9 concentration: 0.5 μM ; final pH: 9.3), and the linear absorbance increase at 350 nm due to the production of *m*-nitrophenol ($\epsilon_{350} = 1140 \text{ M}^{-1}$) was determined. These values were corrected for the background reaction and then used as described above to determine the k_{cat} and K_m values.

Solvent Deuterium Isotope Effects and Buffer Dilution Studies. The steady-state parameters for the hydrolysis of *p*-chloro ester **6c** by NPN43C9 in D₂O were determined in the same manner as described above, with the exception that the buffers were prepared using 99.8% D₂O. The pD values were determined by adding 0.4 to the meter reading.¹²

The rate of hydrolysis of *p*-chloro ester **6c** (400 μM) in the presence and absence of NPN43C9 (0.1 μM) at pH 8.5 was determined as a function of buffer concentration [I (ionic strength) = 0.025–0.2 M] in both H₂O and D₂O. The observed rates of uncatalyzed hydrolysis were plotted versus buffer concentration to give $k_{buff(H)} = 4.2 \pm 0.4 \times 10^{-4} \text{ M}^{-1} \text{ s}^{-1}$ and $k_{buff(D)} = 3.2 \pm 0.2 \times 10^{-4} \text{ M}^{-1} \text{ s}^{-1}$. These rates are corrected for differences in Tris protonation in H₂O ($pK_a = 8.15$) and D₂O ($pK_a = 8.72$). The buffer catalyzed rate is presumably due primarily to nucleophilic attack on the ester by Tris.¹³ The rate of hydrolysis extrapolated to zero buffer concentration (k_{im}) was used to determine $k_{OH} = 8.8 \pm 0.8 \text{ M}^{-1} \text{ s}^{-1}$ and $k_{OD} = 8.4 \pm 0.4 \text{ M}^{-1} \text{ s}^{-1}$ with the following equation: $k_{im} = k_{OH}(K_w/a_H) + k_0$ (assuming that k_0 is negligible).¹⁴ The antibody-catalyzed rate of hydrolysis of **6c** at $I = 0.1 \text{ M}$ was decreased ~25% versus the extrapolated rate at zero buffer concentration.

pH-Rate Profiles. For the *p*-chloro ester **6c**, a full v/S plot was determined at each of 9 pH values. Due to the high K_m values (~3 mM) for the *p*-acetyl ester **6a** and *p*-methyl ester **6d**, k_{cat}/K_m at pH values other than 9.3 was determined directly from the slope of a plot of initial velocity versus $[S]$ at $[S] = 50\text{--}250 \mu\text{M}$. The data obtained were fit to an equation of the form $\log v = \log [C/(1 + H/K_a)]$ (where v and C are, respectively, the pH-dependent and pH-independent values of k_{cat}/K_m) using the Kintastat program.

Hydrolysis of Anilide **9 by NPN43C9.** Initial velocities for the hydrolysis of the *p*-chloroanilide **9** by NPN43C9 were determined by HPLC quantitation of the acid product. The 1-mL reaction mixture contained 2.0 μM monoclonal antibody NPN43C9, 1000 μM of the

(10) (a) Prepared from (4-aminophenyl)acetic acid by treatment with BOC-ON (2-(((*tert*-butoxycarbonyl)oxy)imino)-2-phenylacetoneitrile; Aldrich Chemical Co.) in triethylamine (1 equiv)/DMF: ¹H NMR (360 MHz, CDCl₃) δ 7.32 and 7.18 (two d, AB pattern, *J* ~ 7.5 Hz, 4 H), 6.7–6.5 (br s, 1 H), 3.60 (s, 2 H), 1.50 (s, 9 H). Itoh, M.; Hagiwara, D.; Kamiya, T. *Bull. Chem. Soc. Jpn.* **1977**, *50*, 718–721. Using H₂O/dioxane as solvent (as described in the paper) afforded none of the desired product. (b) We believe analyses of **6b** and **8** were incorrect due to the small amounts of material available for analysis. However, the samples used for antibody assays were pure by ¹H NMR and HPLC.

(11) Cleland, W. W. *Methods Enzymol.* **1979**, *63*, 103–138.

(12) Fife, T. H.; Bruce, T. C. *J. Phys. Chem.* **1961**, *65*, 1079–1080.

(13) Bruce, T. C.; York, J. L. *J. Am. Chem. Soc.* **1961**, *83*, 1382–1387.

(14) Bruce, T. C.; Fife, T. H.; Bruno, J. J.; Benkovic, P. *J. Am. Chem. Soc.* **1962**, *84*, 3012–3018.

anilide **9**, and 5% DMF in ATC buffer, pH 9.0. The mixture was then incubated at 37 °C, and aliquots were removed, quenched to pH ~2 with 23% HClO₄, and analyzed by HPLC. The chromatographic system consisted of a Waters 600E solvent delivery module equipped with a Waters 990 diode array UV-visible detector (monitoring at 254 nm) and a Supelco C-18 reversed phase analytical column (4.6 mm × 25 cm). A flow rate of 1 mL/min was used with a linear gradient of 95% A to 95% B over 30 min (A: 0.1% trifluoroacetic acid in water; B: acetonitrile). The amount of acid **3** produced was determined using a standard curve generated with known amounts of **3**.

Determination of Off Rates by Stopped Flow Fluorescence Studies. In order to determine the rate of dissociation of phenols **7a-d** and ester **6c** from the antibody NPN43C9, a competition experiment was performed wherein the antibody-ligand complex was rapidly mixed with an excess of a tight binding ligand (the *p*-nitrophenol **5**). The rate of dissociation of **7a-d** and **6c** from the antibody was measured by observing the rate of change in intrinsic antibody fluorescence upon binding of **5** to NPN43C9 (phenols **7a-d** cause negligible effects on fluorescence upon binding to NPN43C9). Equal volumes of solution A (1.0 μM antibody and *para*-substituted phenol (concentration = 100–500 μM) or ester **6c** (2000 μM) in 2.5% DMF/ATC) and solution B (*p*-nitrophenol (200–800 μM) in 2.5% DMF/ATC) were rapidly mixed in an Applied Photophysics stopped flow spectrophotometer operating in the fluorescence mode (excitation wavelength = 280 nm). The increase in antibody fluorescence was measured and fit to a single exponential to give the corresponding off rate.

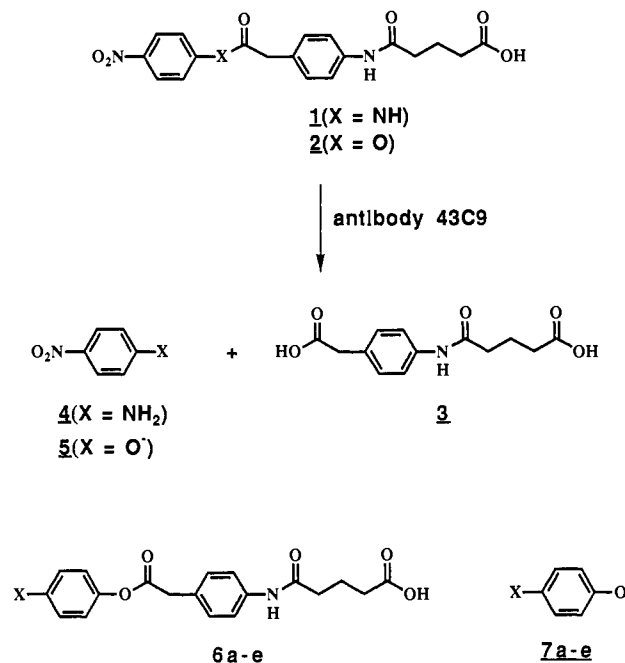
Determination of *K*_d of *m*-Nitrophenol for NPN43C9 by Fluorescence Titration. The quenching of the intrinsic antibody fluorescence at 340 nm as a function of *m*-nitrophenol concentration was determined using a SLM 8000 spectrofluorimeter (excitation wavelength = 280 nm). In a separate control experiment, a known quantity of tryptophan was titrated with *m*-nitrophenol to correct for inner filter effects. The data were then fit as described previously¹⁵ to give a *K*_d value of 14 ± 3 μM.

Pre-Steady-State Hydrolysis of **6b by NPN43C9.** Equal volumes of ester **6b** (2000 μM) in 2.5% DMF/ATC and NPN43C9 (4.0 μM) in 2.5% DMF/ATC were mixed together in an Applied Photophysics stopped flow spectrometer (final substrate concentration: 1000 μM; final NPN43C9 concentration: 2.0 μM; final pH: 7.0 or 8.0), and the absorbance increase at 300 nm due to the production of *p*-hydroxybenzaldehyde **7b** (ε = 15050 M⁻¹) was determined. No burst of phenol product was observed.

Results

Steady-State Parameters and Ligand Binding. Table I displays the kinetic parameters for the hydrolysis of esters **2**, **6a-d**, and **8** by NPN43C9. The unsubstituted phenyl ester **6e** was not a substrate for the antibody. Although the *k*_{cat} values for the alternate substrates are a factor of 10–100 less than that observed for the *p*-nitro ester **2**, the difference in rate acceleration (*k*_{cat}/*k*_{uncat}) is a factor of 10 or less, and thus by this measure the antibody is nearly as efficient a catalyst for the alternate substrates **6a-d** as it is for its "natural" substrate **2**. However, the binding affinities of esters **6a-d** for NPN43C9 as measured by their *K*_m values are much lower than for the *p*-nitro ester, and thus their apparent second-order rate constants (*k*_{cat}/*K*_m) are much lower. The *m*-nitro ester **8** is bound nearly as tightly by the antibody as the *p*-nitro ester **2**, but it is a much poorer substrate for NPN43C9 than any of the other esters studied.

The thermodynamic binding constants (*K*_i or *K*_d) and product dissociation rates (*k*_{off}) for the acid (**3**) and phenol (**5**, **7b**, **7c**) products of the antibody catalyzed hydrolyses are also shown in Table I. Note that in each case, the *K*_d or *K*_i for the phenol is tighter than the apparent *K*_s (*K*_m) for the ester substrate, although the ratio is much less with the alternate substrates **6b**, **6c**, and **8** than with the *p*-nitro ester **2**. For the alternate substrates, the off rates are much higher than the observed *k*_{cat} values. Thus chemistry rather than product desorption is rate limiting at pH > 9 in contrast to the *p*-nitro ester **2**.² Having established that product dissociation was rapid for esters **6a-d**, we looked for direct evidence of an acyl-antibody intermediate via the production of a pre-steady-state burst of phenol product. No burst was seen in the reaction of NPN43C9 with the *p*-formyl ester **6b**; however, we believe this may be due to an unfavorable internal equilibrium (vide infra).



a: X = COCH₃; b: X = CHO; c: X = Cl; d: X = CH₃; e: X = H

Figure 1. Structures of substrates **1**, **2**, and **6a-e**.

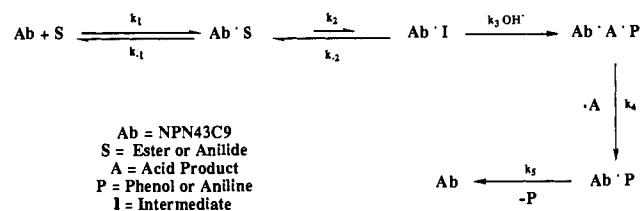


Figure 2. Kinetic mechanism for antibody NPN43C9 (from ref 2).

The variation in *k*_{cat}/*K*_m with pH was determined for the *p*-acetyl ester **6a**, the *p*-chloroester **6c**, and the *p*-methyl ester **6d** (Figures 4 and 5). The apparent p*K*_a shifts from 8.9 for **2** to 9.3 for **6a** and **6c** and 9.5 for **6d** (the p*K*_a in *k*_{cat}/*K*_m for the *p*-nitroanilide **1** is 9.1³). The *k*_{cat}/*K*_m-pH profile for ester **6c** has also been determined in D₂O (Figure 4). An inverse isotope effect was observed in the pH-independent *k*_{cat}/*K*_m value (*C*_H/*C*_D ~ 0.6), and in *k*_{cat} at pH 10.5 (*k*_H/*k*_D ~ 0.7). In contrast, no solvent isotope effect was seen at pH > 9 with the *p*-nitroanilide **1**.³ The apparent p*K*_a in the pH-rate profile shifted from 9.3 in H₂O to 10.0 in D₂O.

Structure-Reactivity Correlation. The fact that a series of five *para*-substituted phenyl esters is efficiently hydrolyzed by NPN43C9 offered an opportunity to determine the electronic effect on the antibody-catalyzed reaction via a Hammett σ - ρ correlation. We investigated the correlation of the rates of ester hydrolysis in the absence of the antibody (pH 9.3, 2.5% DMF/ATC buffer, *I* = 0.1). The original Hammett σ parameters were used for the correlation, with the exception that a value of 1.0, intermediate between the σ value of 0.78 and the σ^- value of 1.27, was used for the *p*-nitrophenyl ester.¹⁶ An excellent correlation was obtained (Figure 6; *R*² = 0.97) which afforded a ρ value of +0.8.

The antibody-catalyzed rates which were used in the σ - ρ correlation were the maximum *k*_{cat} values determined from the pH-rate profiles. We believe this number corresponds to the acylation rate (*k*₂ in Figure 2; vide infra). For the *p*-acetyl and *p*-methyl esters (**6a** and **6d**), the plateau *k*_{cat} value was estimated by multiplying the plateau value for *k*_{cat}/*K*_m by the *K*_m value determined at pH 9.3, and for the *p*-formyl ester **6b** the value was

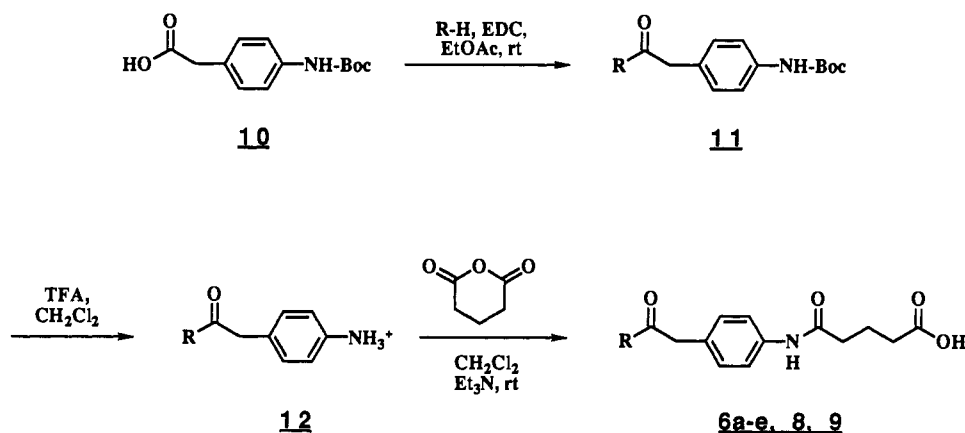
(15) Taira, K.; Benkovic, S. J. *J. Med. Chem.* **1988**, *31*, 129–137.

(16) Bruice, T. C.; Benkovic, S. J. *J. Am. Chem. Soc.* **1964**, *86*, 418–426.

Table I. Kinetic Parameters for Ester Hydrolysis by NPN43C9^a

	X	k_{cat} (s ⁻¹)	K_m (mM)	k_{cat}/K_m (mM ⁻¹ s ⁻¹)	k_{uncat} (s ⁻¹ × 10 ⁴)	K_d or K_i^c (μM)	$k_{\text{off}}^{c,f}$ (s ⁻¹)
2	NO ₂	~25 ^b	0.053 ± 0.019	~470 ^b	9.3	1.0 ± 0.1 ^d	40 ± 5
6a	CH ₃ CO	~0.87 ^b	~3.0	~0.282 ^b	5.1		>700
6b	CHO	1.0 ± 0.1	0.25 ± 0.08	4.1 ± 1.0	2.6	90 ± 10 ^e	>80
6c	Cl	1.7 ± 0.2	0.72 ± 0.22	2.3 ± 0.5	2.4	180 ± 40 ^e	~900
6d	CH ₃	0.15 ± 0.03	~3.0	0.049 ± 0.004	0.93		>700
8	<i>m</i> -NO ₂	0.072 ± 0.01	0.059 ± 0.027	1.01 ± 0.33	4.5	14 ± 3 ^d	~150

^a Measurements were done at pH 9.3 in 2.5% DMF/ATC buffer, $I = 0.1$ (25 °C) unless otherwise noted. ^b Estimate for pH 9.3 based on pH-rate profile. ^c K_d/K_i and k_{off} values are for phenols **5**, **7a-d**, and *m*-nitrophenol. ^d K_d (measured at pH 7.0). ^e K_i (measured at pH 9.5). ^f k_{off} (measured at pH 7.0).



6a: R = *p*AcC₆H₄O; **6b:** R = *p*CHOC₆H₄O; **6c:** R = *p*ClC₆H₄O; **6d:** R = *p*CH₃C₆H₄O;

6e: R = C₆H₅O; **8:** R = *m*NO₂C₆H₄O; **9:** R = *p*ClC₆H₄NH

Figure 3. Synthesis of alternate substrates for NPN43C9.

extrapolated from k_{cat} at pH 9.3 assuming a pK_a of 9.3. The plateau in k_{cat} for the *p*-nitro ester **2** is limited by the *p*-nitrophenol off rate; therefore, the estimated value of 180 s⁻¹ for k_2 was used.² An excellent correlation was again obtained (Figure 6; $R^2 = 0.90$) which afforded a ρ value of +2.3.

The electronic effect on the hydrolysis of anilides by NPN43C9 was also briefly investigated. The hydrolysis of 1000 μM *p*-chloroanilide **9** (estimated to be $\sim K_m$ from the K_m of the *p*-chloro ester **6c** and the fact that the K_m of the amide **1** is $\sim 2 \times$ that of the ester **2**) by the antibody at pH 9.0 was quite slow; however, we were able to estimate a k_{cat} of 0.036 h⁻¹. This value is ~ 80 fold lower than the k_{cat} observed for the *p*-nitroanilide **1** at this pH.

Discussion

Substrate Specificity. Previous studies have shown that catalytic antibodies are highly specific with respect to their substrates. It was demonstrated that NPN43C9 hydrolyzes neither *o*-nitroanilide **13** (Figure 7) nor the saturated analogue of the *p*-nitroanilide **1** (compound **14**).³ The saturated ester **15** and the *m*-nitroanilide **16** also were not substrates but were instead competitive inhibitors ($K_i \approx 800 \mu\text{M}$).⁸ We were thus initially unsure that **6a-e** would be substrates for NPN43C9. In fact, as shown above, five out of the six esters were indeed substrates for the antibody. However, the fact that their K_m values were much higher than for the *p*-nitro ester **2** and that a ten-fold increase in K_m was observed upon substitution of a methyl group (*p*-acetyl ester **6a**) for a hydrogen (*p*-formyl ester **6b**) confirms that the structural requirements of the NPN43C9 binding site for substrates are quite demanding. With another hydrolytic catalytic antibody, it was found that decreased binding (as measured by K_m) of alternate ester substrates led to increased $k_{\text{cat}}/k_{\text{uncat}}$ ratios,¹⁷ but this was not the case with NPN43C9. As noted above, the K_d for the phenol

product is tighter than the K_m for the corresponding ester substrate, although the ratio is much less with the alternate substrates than with the *p*-nitro ester **2**. This tighter binding of the negatively charged phenols may be due to an electropositive environment in the antibody binding site elicited by the negatively charged hapten. This electropositive environment is also presumably responsible for the shift in the pK_a (from ~ 7.1 to ~ 6.0) of *p*-nitrophenol upon binding to NPN43C9.² The only ester not hydrolyzed by NPN43C9 was the unsubstituted phenyl ester **6e**. This suggests that a substituent in the para position is required to orient the substrate for attack by an active site nucleophile. The fact that the *m*-nitroester **8** is bound very tightly by the antibody, yet is a very poor substrate provides further support for this proposition.

Kinetic Mechanism for NPN43C9. The ratio of $k_{\text{cat}}/k_{\text{uncat}}$ should be equivalent to K_m/K_i for a catalytic antibody, provided that the antibody functions, as expected,¹⁸ strictly via transition state stabilization.¹⁹ However, the rate acceleration observed for NPN43C9 is much higher than that expected from transition state theory, suggesting that it employs some form of chemical catalysis in its mechanistic pathway. The pH-rate profiles also implicate an active site functional group. The simplest mechanism would involve the antibody acting as a general base catalyst to facilitate the attack of water on the anilide or ester substrate. However, the lack of a solvent isotope effect at pH > 9 in the hydrolysis of anilide **1** is inconsistent with a general base mechanism. In addition, the binding of the anilide **1** to NPN43C9 is independent of pH² and the pK_a in the pH-rate profile for **1** is ~ 10 in D₂O,³ a shift some 0.5 units greater than expected if the pK_a of ~ 9 in the pH-rate profiles is due simply to the ionization of a group in the active site.^{20,21} Therefore we also considered mechanisms

(18) Jencks, W. P. *Catalysis in Chemistry and Enzymology*; McGraw-Hill: New York, 1969; p 288.

(19) Benkovic, S. J.; Napper, A. D.; Lerner, R. A. *Proc. Natl. Acad. Sci. U.S.A.* **1988**, *85*, 5355-5358.

(17) Janda, K. D.; Benkovic, S. J.; McLeod, D. A.; Schloeder, D. M.; Lerner, R. A. *Tetrahedron* **1991**, *47*, 2503-2506.

Table II. Estimated Rate Constants for NPN43C9^a

	X	k_1 ($\mu\text{M}^{-1} \text{s}^{-1}$)	k_{-1} (s^{-1})	k_{-1}/k_1^b (μM)	k_2^c (s^{-1})	k_{-2}^c (s^{-1})	k_5 (s^{-1})	k_2/k_{-2}	K_1^d
1	NO ₂			~210	0.0022	≥630	500 ± 50	3.5 × 10 ⁻⁵	
2	NO ₂	1.3	25 ± 4	~19	≥180	≥3600	40 ± 5	0.05	0.910
6a	CH ₃ CO			~3000	~1.7	≥1400	>700	0.0012	
6c	Cl	0.15	89 ± 6	~600	~2.2	≥1200	~900	0.0019	0.037
6d	CH ₃			~3000	~0.25	≥1900	>600	0.00013	0.012

^aWe assume that k_3 ($60 \mu\text{M}^{-1} \text{s}^{-1}$) and k_4 ($330 \pm 40 \text{s}^{-1}$) are constant for all substrates since the acyl moiety remains constant (ref 2). ^b K_m (except for 2). ^cCalculated as described in the text. ^d K_1 represents the equilibrium constant for $[\text{AcIm}][p\text{-XC}_6\text{H}_4\text{OH}]/[\text{ImH}][p\text{-XC}_6\text{H}_4\text{OAc}]$ from Gerstein and Jencks (ref 30).

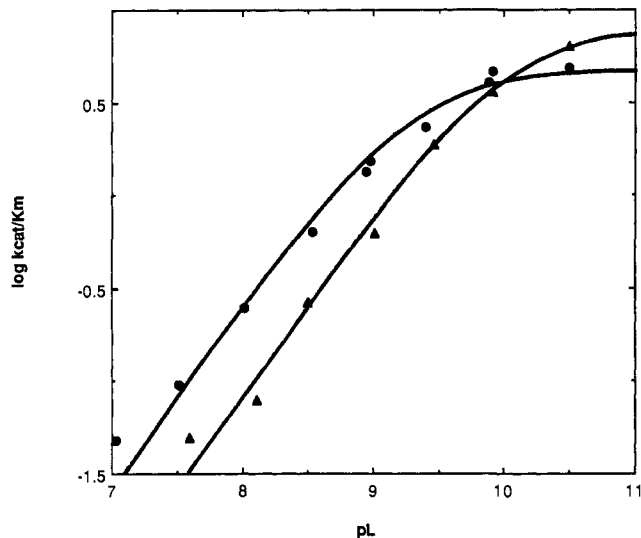


Figure 4. pH- k_{cat}/K_m profiles for the NPN43C9-catalyzed hydrolysis of **6c** in H₂O (●) and D₂O (▲). Solid lines through the data represent nonlinear least-squares fitting according to the equation $\log v = \log [C/(1 + H/K_a)]$.

which involve two chemical steps whose relative rates change with pH.

One possible mechanism would involve changes in the rate-limiting step around a bound tetrahedral intermediate in the antibody binding site which would then lose phenol or aniline to afford products. This tetrahedral intermediate might be generated by rate-limiting water attack at high pH changing to hydroxide assisted expulsion of the leaving group at low pH or by rate-limiting attack by hydroxide ion at low pH changing to rate-limiting protonation of the leaving group in the expulsion step at high pH. The two processes are kinetically indistinguishable and not readily differentiated by solvent isotope effects; either would describe the pH-rate profiles of Figures 4 and 5. In conflict with either version of this mechanism is the absence of exchange of solvent oxygen-18 into the carbonyl of anilide **1**—provided the tetrahedral intermediate can become symmetrical when bound to the antibody.³ Significant isotopic exchange was observed in the uncatalyzed hydrolysis of **1** (which proceeds via a tetrahedral intermediate). Furthermore neither of these mechanisms would give rise to a ρ value >2 for the pH-independent step (vide infra); rate-limiting water attack to form the intermediate would reflect a smaller electronic effect on the carbonyl carbon ($\rho \sim 1.2$),²²⁻²⁴ and its rate limiting decomposition via the oxygen- or nitrogen-protonated species is subject to a cancellation of effects.²⁵ In addition, the

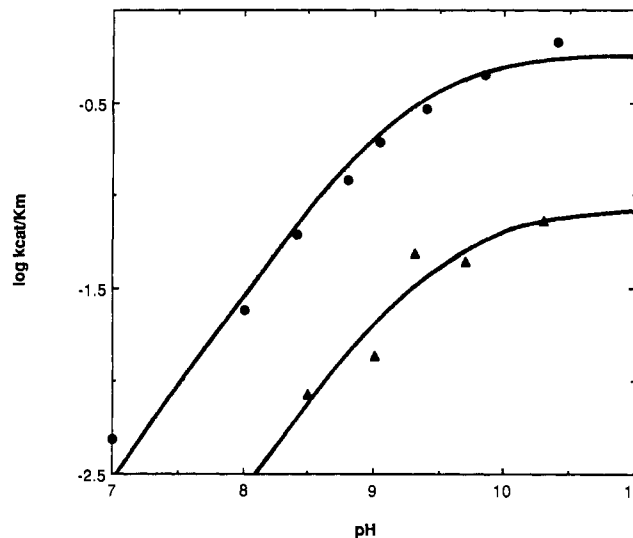


Figure 5. pH- k_{cat}/K_m profiles for the NPN43C9-catalyzed hydrolyses of **6a** (●) and **6d** (▲). Solid lines through the data represent a nonlinear least-squares fitting according to the equation $\log v = \log [C/(1 + H/K_a)]$.

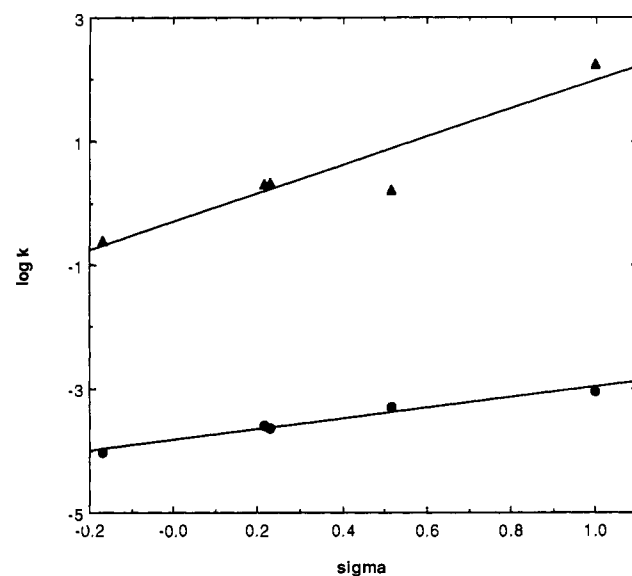


Figure 6. Hammett σ - ρ correlation for the buffer catalyzed (●) and NPN43C9 catalyzed (▲) hydrolyses of esters **2** and **6a-d**. σ values: *p*-NO₂ (**2**), 1.00; *p*-CH₃CO (**6a**), 0.52; *p*-Cl (**6c**), 0.23; *p*-CHO (**6b**), 0.22; *p*-CH₃ (**6d**), -0.17.

hydrolysis of esters by water is characterized by a very large normal isotope effect, in contrast to the isotope effects seen in the pH-independent region.²⁶

A third possible mechanism would involve the rapid yet unfavorable formation of an acyl-antibody intermediate in a pH-independent step, followed by its rapid hydrolysis in a pH-dependent step to afford products (Figure 2). The rate equations

(20) Schowen, K. B.; Schowen, R. L. *Methods Enzymol.* **1982**, *87*, 551-606.

(21) Cleland, W. W. *Adv. Enzymol. Rel. Areas Mol. Biol.* **1977**, *45*, 273-387.

(22) Bruice, T. C.; Schmir, G. L. *J. Am. Chem. Soc.* **1957**, *79*, 1663-1667.

(23) From the data of Moffat and Hunt we were able to estimate a ρ value of 1.3: Moffat, A.; Hunt, H. *J. Am. Chem. Soc.* **1959**, *81*, 2082-2086.

(24) Klinman and Thornton demonstrated that the rates of hydrolysis of substituted benzoylimidazoles by hydroxide and water are equally sensitive to substituent effects: Klinman, J. P.; Thornton, E. R. *J. Am. Chem. Soc.* **1968**, *90*, 4390-4394.

(25) Bender, M. L.; Thomas, R. J. *J. Am. Chem. Soc.* **1961**, *83*, 4183-4189.

(26) Johnson, S. L. *Adv. Phys. Org. Chem.* **1967**, *5*, 312-318.

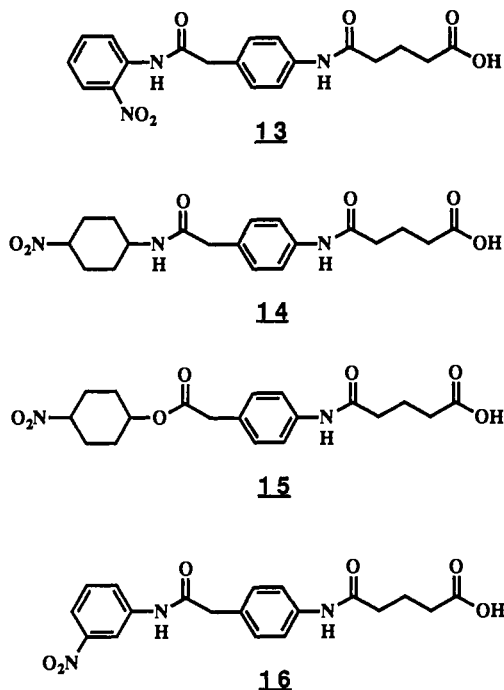


Figure 7. Amides and esters which were not substrates for NPN43C9.

for this mechanism have been derived previously² and are shown in Figure 8. Since we have determined the dissociation rates for the products (k_4 and k_5), the ratio of k_{-1}/k_1 (K_m), and the pH dependence of k_{cat}/K_m , we were able to estimate the values of the rate coefficients for the hydrolysis of **6a-d** by NPN43C9 in the same manner as described previously.² The term k_{cat} ($\text{pH} > 9$) does not equate with the rate of product release of the phenols **7a-d** (k_5), in contrast to the hydrolysis of the *p*-nitro ester **2**. Thus this rate was assigned to the rate of acylation of the antibody by the ester (k_2). Assuming that the rate of deacylation (k_3) remains constant (since the acyl portion of the ester remains constant), we were able to estimate k_{-2} for each ester by substitution into the expression for k_{cat}/K_m ($\text{pH} < 9$). The calculated values for the kinetic constants for amide **1** and esters **2**, **6a**, **6c**, and **6d** are shown in Table II.

The solvent deuterium isotope effects on the pH-rate profiles for anilide **1** and *p*-chloroester **6c** (Figure 4) can be interpreted in terms of the acyl-antibody mechanism as being due to the lack of a solvent isotope effect at high pH but the presence of one at low pH. In general, hydrolysis of esters via a general base mechanism is characterized by a large k_H/k_D of $\sim 2-3$, while hydrolysis via a nucleophilic mechanism exhibits a k_H/k_D of ~ 1 .^{27,28} A k_H/k_D value of $\sim 2-3$ has been observed in the general base assisted acylation of chymotrypsin and subtilisin.²⁹⁻³² However, solvent isotope effects of < 2 have been observed in the acylation of chymotrypsin and trypsin by nonspecific ester substrates, suggesting that these substrates may initially acylate the histidine of chymotrypsin rather than the serine.³³⁻³⁵ The acylation of the antibody (rate-limiting at high pH) should exhibit no solvent isotope effect if it occurs via nucleophilic attack, while the deacylation (rate-limiting at low pH) might exhibit a sig-

$$k_{cat} = \frac{k_2 k_3 k_4 k_5 \text{OH}^-}{k_3 \text{OH}^- [k_4 k_5 + k_2 (k_4 + k_5)] + k_4 k_5 (k_2 + k_{-2})}$$

$$\frac{k_{cat}}{K_m} = \frac{k_1 k_2 k_3 \text{OH}^-}{k_3 \text{OH}^- (k_2 + k_{-1}) + k_{-1} k_{-2}}$$

$$K_m = \frac{[k_3 \text{OH}^- (k_2 + K_{-1}) + k_{-1} k_{-2}] k_4 k_5}{k_1 [k_3 \text{OH}^- (k_4 k_5 + k_2 k_4 + k_2 k_5) + k_4 k_5 (k_2 + k_{-2})]}$$

At low pH:

$$k_{cat}(\text{pH} < 9) = \frac{k_2 k_3 \text{OH}^-}{k_2 + k_{-2}}$$

$$k_{cat}/K_m(\text{pH} < 9) = \frac{k_1 k_2 k_3 \text{OH}^-}{k_{-1} k_{-2}}$$

At high pH:

$$k_{cat}(\text{pH} > 9) = \frac{k_2 k_4 k_5}{k_4 k_5 + k_2 (k_4 + k_5)}$$

$$k_{cat}/K_m(\text{pH} > 9) = \frac{k_1 k_2}{k_2 + k_{-1}}$$

Figure 8. Rate equations for NPN43C9 (from ref 2).

nificant isotope effect. The observation of a small inverse isotope effect at $\text{pH} > 10$ with ester **6c** was unexpected, but it confirms that the antibody does not function via a simple general base mechanism. The shift of ~ 0.7 in the apparent $\text{p}K_a$ for **6c** (larger than the value of ~ 0.5 expected for normal bases)²⁰ could be due to an isotope effect on general acid assisted hydroxyl attack in the deacylation step, an unusually large D_2O effect on the ionization of a base in the antibody binding site whose $\text{p}K_a$ is outside our observational pH range, or a combination of these two effects.

Further evidence for the acyl-antibody mechanism is provided by the substituent effect observed for the hydrolysis of esters **2** and **6a-d** by NPN43C9. Hydrolysis of phenyl esters via a general base mechanism is characterized by little charge buildup on the phenol oxygen and thus a low ρ value of $0.5-0.7$.^{16,36} Nucleophilic attack by an anionic oxygen nucleophile such as hydroxide is characterized by greater charge buildup in the transition state and thus a higher ρ value of $\sim 1.0-1.2$.^{22,36,37} The ρ value of 0.8 which was observed in the hydroxide-buffer catalyzed hydrolysis of esters **2** and **6a-d** is consistent with these previous observations. However, the ρ value of 2.3 observed in the NPN43C9 catalyzed reaction is significantly different than the value expected for a general base catalyzed reaction. A large ρ value of $2-3$ in the hydrolysis of phenyl esters is characteristic of nucleophilic attack by a neutral nitrogen nucleophile, such as imidazole.^{16,22,36} Thus the substituent effect provides evidence for an acyl intermediate and against a one step general base mechanism.

Several structure-reactivity studies have been performed on the hydrolysis of phenyl esters by serine proteases. In studies employing specific amino acid phenyl esters, ρ values of $0-0.63$ have been observed, consistent with the view that acylation of chymotrypsin and subtilisin occurs via general base assisted attack by the hydroxyl group of a serine residue.^{32,38-40} The second order

(27) Anderson, B. M.; Cordes, E. H.; Jencks, W. P. *J. Biol. Chem.* **1961**, *236*, 455-463.

(28) Bender, M. L.; Pollock, E. J.; Neveu, M. C. *J. Am. Chem. Soc.* **1962**, *84*, 595-599.

(29) Bender, M. L.; Hamilton, G. A. *J. Am. Chem. Soc.* **1962**, *84*, 2570-2576.

(30) Bender, M. L.; Clement, G. E.; Kezdy, F. J.; Heck, H. d'A. *J. Am. Chem. Soc.* **1964**, *86*, 3680-3690.

(31) Bundy, H. F.; Moore, C. L. *Biochemistry* **1966**, *5*, 808-811.

(32) Matta, M. S.; Greene, C. M.; Stein, R. L.; Henderson, P. A. *J. Biol. Chem.* **1976**, *251*, 1006-1008.

(33) Hubbard, C. D.; Kirsch, J. F. *Biochemistry* **1972**, *11*, 2483-2493.

(34) Hubbard, C. D.; Shoupe, T. S. *J. Biol. Chem.* **1977**, *252*, 1633-1638.

(35) Elrod, J. P.; Hogg, J. L.; Quinn, D. M.; Venkatasubban, K. S.; Schowen, R. L. *J. Am. Chem. Soc.* **1980**, *102*, 3917-3922.

(36) Bruice, T. C.; Mayahi, M. F. *J. Am. Chem. Soc.* **1960**, *82*, 3067-3071.

(37) Kirsch, J. F.; Clewell, W.; Simon, A. *J. Org. Chem.* **1968**, *33*, 127-132.

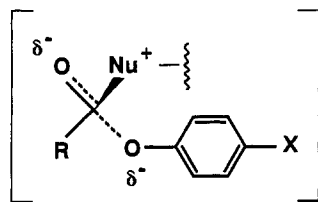


Figure 9. Postulated rate-limiting transition state for acylation of NPN43C9.

rate of acylation of chymotrypsin by nonspecific phenyl esters is much more susceptible to substituent effects ($\rho = 1.4\text{--}2.0$) and this has been taken as evidence that these substrates initially acylate the imidazole of the catalytic histidine rather than the serine hydroxyl.^{33,34,41} However, other studies have presented conflicting data on the hydrolysis of nonspecific esters.^{42,43} Since substrates **2** and **6a-d** are highly homologous with the hapten used to induce the antibody, we believe that our results should be compared to the results obtained with the specific ester substrates of chymotrypsin and trypsin, and are thus indicative of a much higher charge buildup in the transition state for the antibody-catalyzed reaction. Fersht has argued that k_{cat}/K_m rather than k_{cat} should be employed in structure-reactivity studies.⁴⁴ Although we believe that the plateau k_{cat} values correspond to k_2 (vide supra), and thus their use in a $\sigma\text{--}\rho$ correlation is appropriate, it should be noted that a correlation of the plateau k_{cat}/K_m values with σ also affords a very high ρ value ($\rho = 3.2$, $R^2 = 0.74$).

The results of the substituent effect study suggest that the antibody nucleophile acylated by the substrate may be the imidazole group of a histidine residue. While there is little enzymatic precedent for nucleophilic attack by an imidazole, other lines of evidence indicate that this mechanism may be operative. There are two histidines in the complementary determining regions of the antibody combining site,⁹ and molecular modeling experiments (Roberts, V. A., unpublished data) suggest that one may be in the proper orientation for nucleophilic attack on the carbonyl of the substrate. The imidazole of a histidine should be in its neutral form (and thus active as a nucleophile) in the pH range investigated (7.0–10.5), and this would explain our inability to observe a second apparent $\text{p}K_a$ due to ionization of the antibody nucleophile. Out of a series of classical chemical modification reagents, diethyl pyrocarbonate (which specifically inactivates histidines) was the only one which inactivated NPN43C9 (Borders, C. L., Jr., unpublished results). Furthermore, the internal equilibrium (k_2/k_{-2}) observed is similar to what one would expect for the attack of an imidazole on an ester from the studies of Jencks on the reaction of imidazole with substituted phenyl acetates (Table II).^{45,46} We believe the more unfavorable internal equilibrium seen for ester **2** compared to that expected from Jencks' value may result from the tight binding of *p*-nitrophenol to the antibody.

The interpretation of the $\text{p}K_a$ in the pH-rate profile as resulting from a change in rate limiting step (from deacylation to acylation or product release) implies that it should shift as the substituent changes due to a change in the relative rates of these steps. The $\text{p}K_a$ did indeed shift, but the change seen was fairly modest (from 8.9 to 9.5), and the result was not as definitive as we had hoped

for. If one sets the equations for k_{cat}/K_m ($\text{pH} < 9$) and k_{cat}/K_m ($\text{pH} > 9$) equal to each other, then (assuming that $k_{-1} \gg k_2$, which is true for **6c**) $k_3[\text{OH}^-] \approx k_{-2}$ and thus $\Delta\text{p}K_a \approx \log(\Delta k_{-2})$. Therefore the small shift in the apparent $\text{p}K_a$ indicates that k_{-2} does not change significantly as the phenol nucleophile is changed. The small change in k_{-2} could be the result of a late transition state in the acylation reaction (consistent with the high ρ value observed). This would then result in an early transition state (and thus an attenuation of the substituent effect) for the reverse deacylation reaction, and the lack of a correlation of k_{-2} with σ .

Finally, we address the degree of bond cleavage of the departing aniline or phenol in the acylation reaction. The lack of a solvent isotope effect on acylation and the high ρ value observed both indicate that protonation of the leaving group either does not occur or lags behind bond cleavage. We attribute much if not all of the ρ value to electronic effects arising in the transition state; the lack of a correlation of K_m with σ argues against the importance of hydrophobic effects on binding stemming from the para substituent.⁴⁷ A postulated view of this transition state is shown in Figure 9. Particularly intriguing is the fact that the rate of hydrolysis of the *p*-chloroanilide **9** by NPN43C9 is ~ 80 times slower than that observed for the *p*-nitroanilide **1**. This is in sharp contrast to the results obtained for the hydrolysis of anilides by chymotrypsin, wherein no clear substituent effect was observed,⁴⁸ presumably due to the fact that protonation of the anilide leaving group (which should have a negative ρ value) occurs simultaneously with expulsion of the group from the tetrahedral intermediate.²⁵ The expulsion of a fully ionized anilide from the tetrahedral intermediate in the acylation of the antibody appears unlikely; however, it has been shown that *p*-nitroacetanilide and *p*-nitrotrifluoroacetanilide hydrolyze in basic aqueous solutions ($\text{pH} > 9$) via a mechanism which involves loss of the *p*-nitroanilide anion.^{49,50}

Conclusion

Three types of evidence (solvent isotope effect studies, substituent effect studies, and pH-rate studies) have been presented in this paper which all indicate that antibody NPN43C9 hydrolyzes its substrates via a covalent acyl-antibody intermediate. It is unexpected that an antibody induced by a single transition state analogue would carry out its hydrolytic action via two transition states. This antibody exhibits both surprising similarities to and striking differences from naturally occurring hydrolytic enzymes, further supporting our view that catalytic antibodies may provide a view of how primitive, nonoptimized enzymes may have functioned. Efforts are underway in our laboratory to explore further the mechanism of NPN43C9 employing site-directed mutagenesis.

Acknowledgment. This work was supported in part by NIH Grant GM4385801 to K.D.J. and by NSF Fellowship CHE-8808377 to R.A.G. We thank M. I. Weinhouse, D. A. McLeod, and D. M. Schloeder for expert technical assistance and J. A. Adams for assistance with the initial phases of this project and many stimulating discussions.

Registry No. **1**, 117746-37-9; **6a**, 139631-79-1; **6b**, 139631-80-4; **6c**, 135713-18-7; **6d**, 139631-81-5; **6e**, 139631-82-6; **8**, 139631-83-7; **9**, 139631-84-8; **10**, 81196-09-0; **12** (R = *p*-AcC₆H₄O), 139631-73-5; **12** (R = *p*-CHOC₆H₄O), 139631-74-6; **12** (R = *p*-ClC₆H₄O), 139631-75-7; **12** (R = *p*-MeC₆H₄O), 139631-76-8; **12** (R = PhO), 139631-77-9; **12** (R = *m*-NO₂C₆H₄O), 139655-34-8; **12** (R = *p*-ClC₆H₄NH), 139631-78-0; *p*-acetylphenol, 99-93-4; *p*-formylphenol, 123-08-0; *p*-chlorophenol, 106-48-9; *p*-methylphenol, 106-44-5; phenol, 108-95-2; *m*-nitrophenol, 554-84-7; *p*-chloroaniline, 106-47-8; deuterium, 7782-39-0; glutaric anhydride, 108-55-4.

(47) Fastrez, J.; Fersht, A. R. *Biochemistry* **1973**, *12*, 1067–1074.

(48) Philipp, M.; Pollack, R. M.; Bender, M. L. *Proc. Natl. Acad. Sci. U.S.A.* **1973**, *70*, 517–520.

(49) Pollack, R. M.; Bender, M. L. *J. Am. Chem. Soc.* **1970**, *92*, 7190–7194.

(50) Pollack, R. M.; Dumsha, T. C. *J. Am. Chem. Soc.* **1973**, *95*, 4463–4465.

(38) Williams, A. *Biochemistry* **1970**, *9*, 3383–3390.

(39) Williams, R. E.; Bender, M. L. *Can. J. Biochem.* **1971**, *49*, 210–217.

(40) Williams, A.; Woolford, G. *J. Chem. Soc., Perkin Trans. II* **1972**, 272–275.

(41) Bender, M. L.; Nakamura, K. *J. Am. Chem. Soc.* **1962**, *84*, 2577–2582.

(42) Dupaix, A.; Bechet, J.-J.; Roucoux, C. *Biochemistry* **1973**, *12*, 2559–2566.

(43) Ikeda, K.; Kunugi, S.; Ise, N. *Arch. Biochem. Biophys.* **1982**, *217*, 37–46.

(44) Fersht, A. *Enzyme Structure and Mechanism*; 2nd ed.; W. H. Freeman and Company: New York, 1985; pp 87–88.

(45) Kirsch, J. F.; Jencks, W. P. *J. Am. Chem. Soc.* **1964**, *86*, 837–846.

(46) Gerstein, J.; Jencks, W. P. *J. Am. Chem. Soc.* **1964**, *86*, 4655–4663.